

Stochastic parallel gradient descent laser beam control algorithm for atmospheric compensation in free space optical communication



Jingtai Cao ^{a,b}, Xiaohui Zhao ^{a,*}, Zhaokun Li ^a, Wei Liu ^a, Yang Song ^{b,c}

^a College of Communication Engineering, Jilin University, 5372 Nanhu Road, Changchun 130012, China

^b Changchun Institute of Optics, Fine Mechanics and Physics, Chinese Academy of Sciences, 3888 Nanhu Road, Changchun 130033, China

^c Graduate School of Chinese Academy of Sciences, Beijing 100039, China

ARTICLE INFO

Article history:

Received 5 November 2013

Accepted 4 June 2014

Keywords:

FSO communication

Atmospheric compensation

Fiber coupling

SPGD

ABSTRACT

Atmospheric turbulence seriously degrades the performance of free space optical (FSO) communication systems, especially the coupling efficiency. In this paper, we propose a stochastic parallel gradient descent (SPGD) algorithm to compensate the atmospheric turbulence in FSO communication system. Theoretical analysis and work flow of the algorithm are given. Both simulation and experimental results indicate that the coupling efficiency can be increased from 12% to more than 80% after 270 iterations or more than threefold, which implies a significant improvement of the performance.

© 2014 Elsevier GmbH. All rights reserved.

1. Introduction

It is quite well known that the study of FSO systems is increasingly important and significant, owing to its advantages over RF (or millimeter-wave) systems such as improved security, no spectrum licensing, and faster speed over the short-haul access [1–7]. However, due to its narrow beam divergence angle, FSO communication systems are generally extremely sensitive to atmospheric turbulence and mechanical vibration. And atmospheric turbulence [8–10,6,11] is the major impairment which causes variation of atmosphere refractive index with time and space, and with both amplitude and phase of laser signal fluctuating along its propagation path [12]. This leads to serious degradation for the performance of free space optical (FSO) communication systems, while the coupling efficiency suffers most [13–16]. Generally, adaptive optics (AO) is acknowledged as an effective method to compensate the atmospheric turbulence [17–21].

Most current AO systems concerned about wave-front phase distortion. Shack–Hartmann wave-front sensor (SH-WFS) is a typical sensor used in AO systems. But it has flaws in FSO systems applications in which the intensity cannot be all time detected, due to the scintillation effect. Especially when it comes to near-ground remote transmission, the laser scintillation from atmospheric turbulence is tremendous [22,23]. A new wave-front measurement

method based on focal plane which can avoid power loses by less spectroscopic is proposed [24]. Nevertheless, these methods usually concentrate on phase distortion.

The conventional adaptive optics systems are based on wave-front conjugation principle, and phase conjugation is realized in an optoelectronic feedback-loop system comprising wave-front sensor and reconstructor. The system usually uses a single deformable mirror or other phase correction device to compensate phase distortion. The compensation performance of AO system largely depends on the characteristics of the deformable mirror (DM) and is limited by the stroke and the spatial frequency of actuators. Recently, sensor-less measurement technology algorithms used in AO systems [25,26] have been developed, in which the wave-front correctors need some information that associated with the wave-front aberrations as the feedback and control parameter of the correction element. In this paper, we propose a new atmospheric compensation method based on SPGD algorithm. In order to testify the feasibility of our method, the numerical simulation of compensation process of random atmospheric turbulence is given, and the analysis of the fiber coupling efficiency before and after compensation is provided. A closed-loop laboratory experimental system is built up, in which the deformable mirror (DM) is real-time manipulated by an embedded controller with parallel processing technology and the atmospheric turbulence is simulated by a turbulence simulation box. The results of the repeated experiments show that the proposed method can compensate efficiently the atmospheric turbulence and significantly improve fiber coupling efficiency.

* Corresponding author. Tel.: +86 431 85152181; fax: +86 431 85152181.

E-mail address: xhzhao@jlu.edu.cn (X. Zhao).

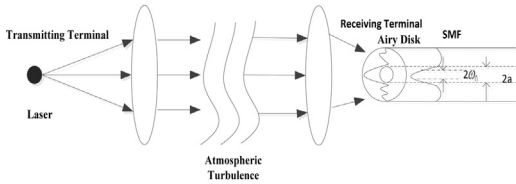


Fig. 1. Functional block diagram of FSO systems.

The structure of this paper is as follows. In Section 2, we describe the model of the system and the principle of the proposed algorithm. In Section 3, the efficiency analysis of the FSO system is provided. In Section IV, the wave-front distribution during the iteration through numerical simulation is discussed, with the coupling efficiency before and after compensation to verify the feasibility of our proposed algorithm. Finally, we set up a closed-loop FSO communication experimental system, where the deformable mirrors (DMs) are real-time manipulated by an embedded controller with parallel processing technology, and the atmospheric turbulence is simulated by a turbulence simulation box.

2. Numeral model of SPGD algorithm

2.1. System model

The functional block diagram of FSO communication systems is shown in Fig. 1, including transmitting terminal, atmospheric channel and receiving terminal. As shown in Fig. 1, atmospheric scintillation occurs due to thermally induced refractive index changes of the air along the optical link, causing rapid fluctuation of signal irradiance at the receiver, reduction in degree of coherence of the optical signal [2], and potentially poor bit error rate (BER), seriously affects the performance of FSO systems in single mode fiber (SMF).

2.2. Actuator model

Based on clear aperture and separation distances between the actuators in the unit circle, we configure the normalized layout of 32-element deformable mirrors (DMs) actuators, as shown in Fig. 2. The influence function of the actuators on each point in the unit circle can be approximated by Gaussian function

$$S_j(x, y) = \exp \left\{ \ln \omega \left[\frac{1}{d} \sqrt{(x - x_j)^2 + (y - y_j)^2} \right]^\alpha \right\} \quad (1)$$

where $S_j(x, y)$ is the influence function of j th actuator, (x_j, y_j) is the position coordinate of j th actuator ($j = 1, 2, \dots, 32$). ω is the

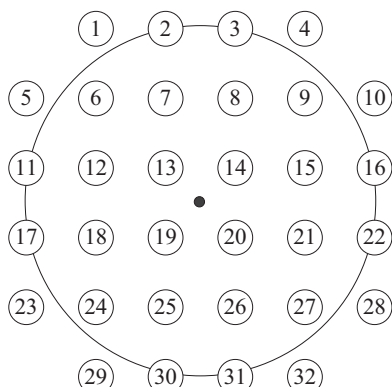


Fig. 2. Layout of 32-element deformable mirrors actuators.

cross-linked value of the actuators usually set to 0.08. d is the normalized distance taken as 0.383. α is the Gaussian index set to 2.

The phase compensation $u(x, y)$ generated by the deformable mirrors is

$$u(x, y) = \sum_{j=1}^{32} v_j S_j(x, y) \quad (2)$$

where v_j is j th voltage of the actuators.

2.3. Model of SPGD algorithm in wave-front distortion correction

The SPGD algorithm [27,28] is an adaptive technique for optical correction based on the simultaneous perturbation stochastic approximation (SPSA) method. It is easy to realize and can concurrently control the parameters calculation.

Normally, The SPGD algorithm in AO systems can be treated as an optimal control problem, whose numeral model is given by

$$\begin{aligned} & \min J[u(r)] \\ & \text{s.t. } \phi_{k+1}(r) = f(\phi_k(r), u(r)), \quad \phi_0(r) = \varphi(r) \end{aligned} \quad (3)$$

where $J[u(r)]$ is the object function describing the relationship between performance metric J and control variable $u(r)$. In AO wave-front distortion correcting systems, we select Strehl ratio as the performance metric J , the phase compensation generated by the wave-front corrector as control variable $u(r)$, and the residual phase difference after k th iteration as state variable $\phi_k(r)$. Naturally, the state equation can be expressed as

$$\phi_{k+1}(r) = \phi_k(r) + u(r) \quad (4)$$

The relationship between SR and $u(r)$ is

$$SR = 1 - \frac{1}{S} \iint_S (\phi_{k+1}(r) - \bar{\phi}_{k+1}(r))^2 r d^2 r \quad (5)$$

$$\phi_{k+1}(r) = \phi_k(r) + u(r) \quad (6)$$

where $\phi_k(r)$ can be measured by the images after iterations. $\bar{\phi}_{k+1}(r)$ is the average of $\phi_k(r)$ on the unit circle.

The initial state $\phi_0(r)$ is the initial wave-front distortion. In the following simulations, we express $\phi_0(r)$ by 3rd to 10th Zernike polynomials [29]

$$\phi_0(r) = \varphi(r) = \sum_{i=3}^{10} \alpha_i Z_i(r) \quad (7)$$

2.4. SPGD algorithm flow

The fundamental principle of SPGD algorithm can be described as

$$\mathbf{v}^{(k+1)} = \mathbf{v}^{(k)} + \gamma \Delta \mathbf{v}^{(k)} [J_+ - J_-] \quad (8)$$

$$J_+ = J[\mathbf{v}^{(k)} + \Delta \mathbf{v}^{(k)}] \quad (9)$$

$$J_- = J[\mathbf{v}^{(k)} - \Delta \mathbf{v}^{(k)}] \quad (10)$$

where γ is the positive gain coefficient. $\Delta \mathbf{v}^{(k)} = [\Delta v_1^{(k)}, \Delta v_2^{(k)}, \dots, \Delta v_{32}^{(k)}]^T$ is the random disturbance vector with independent element $\Delta v_i^{(k)}$ at k th iteration.

$\mathbf{v}^{(k)} = [v_1^{(k)}, v_2^{(k)}, \dots, v_{32}^{(k)}]^T$ is the voltage vector applied to the actuators at k th iteration. $J = J[\mathbf{v}]$ can be obtained by Eqs. (1), (2), (5), and (6). Hence, the SPGD Algorithm flow is described as follows

- a. Get fitted value of wave-front distortion from (7);
- b. Initialize voltage vector $\mathbf{v}^{(0)} = [\nu_1^{(0)}, \nu_2^{(0)}, \dots, \nu_{32}^{(0)}]^T$;
- c. Obtain initial performance metric J taken as SR;
- d. Generate stochastic disturbance $\Delta\mathbf{v}^{(k)} = [\Delta\nu_1^{(k)}, \Delta\nu_2^{(k)}, \dots, \Delta\nu_{32}^{(k)}]^T$;
- e. Obtain $\mathbf{v}^{(k+1)}$ by $\mathbf{v}^{(k)}$ according to Eqs. (8)–(10);
- f. Obtain J at each iteration k and if J satisfies the terminal condition, end the iteration; if not, return to step d. Note that the terminal condition is not unique, it depends on the actual systems.

3. Analysis of fiber coupling efficiency

Generally, the received laser signals are coupled into a single mode fiber, so that the coupling efficiency of single mode fiber, defined as the ratio of the average power coupled into the fiber to the average power in the receiver aperture plane [30], has significant influence on the performance of FSO system. The coupling efficiency can be expressed as

$$J \propto \frac{\left| \iint A_f(r) M_0^*(r) d^2r \right|^2}{\iint A_f(r) A_f^*(r) d^2r \times \iint M_0(r) M_0^*(r) d^2r} \quad (11)$$

where $A_f(r)$ is Fourier transform of the single-mode fiber optical field, $M_0(r)$ is the incident optical field in the focal plane, and $A_f(r)$ and $M_0(r)$ are complex quantities. Since Eq. (11) is too complicated to calculate, we apply Strehl Ratio to simplify the average coupling efficiency [31] given by

$$ST \propto |A_f(r_0)|^2 \quad (12)$$

where r_0 is the desired on-axis location of the center of the fiber. In this paper, we calculate Strehl Ratio of the laser signal images in the focal plane to analyze the coupling efficiency.

4. Numerical simulation

In order to verify the feasibility of our algorithm, numerical simulation is carried out. First we introduce wave-front with Zernike aberrations with the gain coefficient and the initial voltage for DMs settled. Then through several iterations, we observe the wavefront distribution to obtain the coupling efficiency though calculation of the SR during the iteration, and to analyze the performance of atmospheric compensation. During the simulation process, we take the parameters as follows

The coefficient of Zernike polynomials: $\alpha_3 = 1.3$, $\alpha_4 = 0.65$, $\alpha_5 = -0.4$, $\alpha_6 = 0.32$, $\alpha_7 = -0.45$, $\alpha_8 = -0.3$, $\alpha_9 = 0.25$, $\alpha_{10} = -0.15$. We take the gain coefficient $\gamma = 0.8$, and initial voltage vector $\mathbf{v}^{(0)} = [1, 1, \dots, 1]^T$. Each element of the random disturbance vector $\Delta\mathbf{v}$ is independent and is subject to Bernoulli distribution, and $|\Delta\nu_i| = \delta = 0.25$.

According to the principle of the proposed algorithm, we select SR as the performance metric J with initial value 0.12. The results are as Fig. 3 where Fig. 3(a) is the introduced wavefront distribution before correction. Fig. 3(b)–(h) are the residual wavefront distribution after 10 to 350 iterations respectively.

Through calculation of SR, the performance metric J increases from 0.12 to 0.81, which indicates that SPGD algorithm has a significant effect on the atmospheric compensation and improves the performance of FSO communication systems.

We summarize the performance metric $J(\text{SR})$ variation with the number of iteration in Fig. 4. Fig. 4 shows that the performance metric $J(\text{SR})$ increases with the number of iteration N , and it converges to 81% when N is about 270.

The influence of gain coefficient on the convergence of the proposed algorithm is shown in Fig. 5, from which it is obvious that different gain coefficients lead to different rate of convergence.

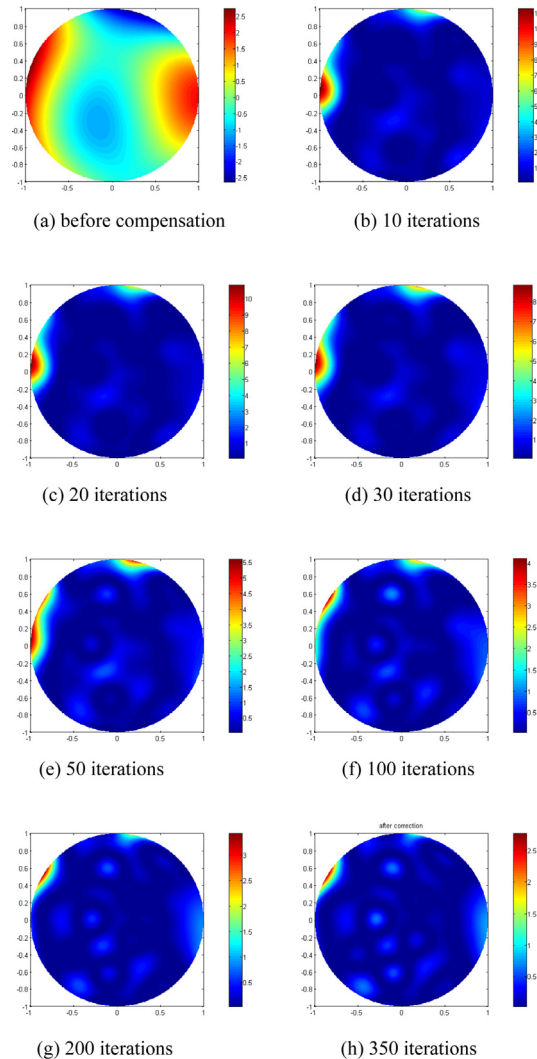


Fig. 3. Residual phase differences after different iterations.

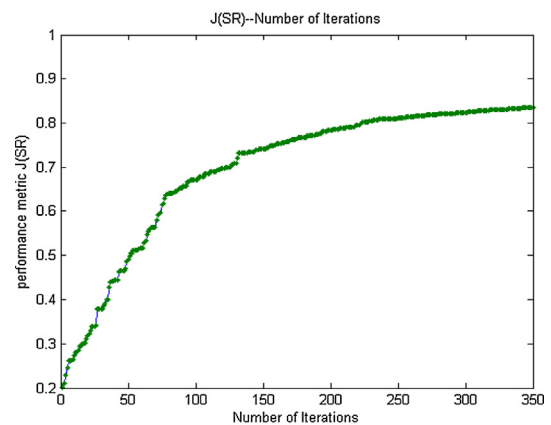


Fig. 4. Performance metric $J(\text{SR})$ with respect to number of iterations (N).

5. Experiment and analysis

To deeply implement and analyze the proposed algorithm, we set up a FSO experiment communication system shown in Fig. 6, with our proposed SPGD algorithm to compensate the atmospheric turbulence in close-loop perspective. There is no wave-front

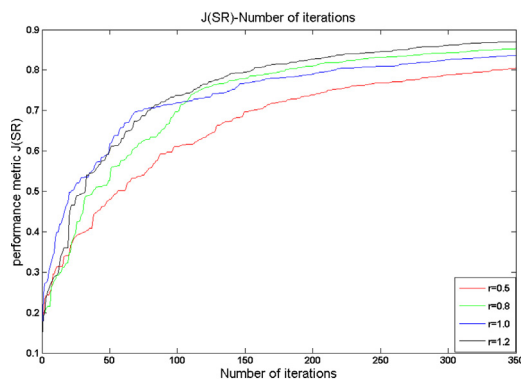


Fig. 5. Influence of gain coefficients on convergence of the algorithm.

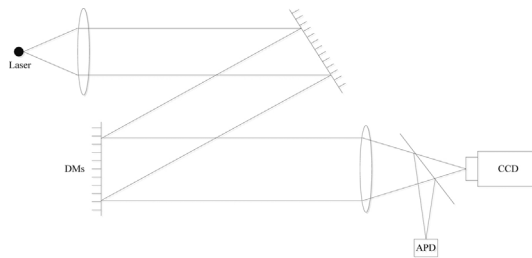


Fig. 6. Diagram of experiment system.

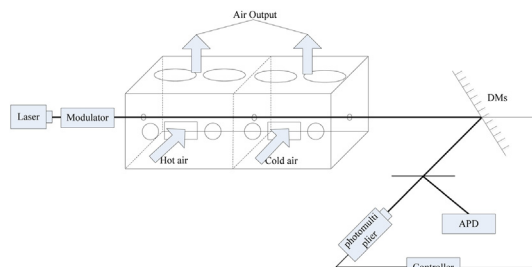


Fig. 7. Structure of FSO experiment communication system.

sensor, and at each iteration, SPGD beam controller is based on some information as the feedback of the correction element.

For the simulation of the atmospheric turbulence, we design an atmospheric turbulence simulation box (ATSB) to simulate atmospheric flow and diffusion shown in Figs. 7 and 8 respectively. Our experiment system contains laser, OOK modulator, ATSB, DMs, CCD camera, photomultiplier, parallel processor, and DMs controller.

The OOK modulated laser beam is sent through ATSB then passes through the turbulence box which can simulate atmospheric turbulence by introducing cold and hot air. It is divided into two beams after passing through DMs, one of them is sent to APD for demodulation so that the communication completes. In order to improve the



Fig. 8. Photo of FSO experiment communication system.



Fig. 9. Image before compensation.



Fig. 10. Image after compensation.

performance of the FSO system, the other beam will be processed by a DM controller to compensate atmospheric turbulence.

To improve system efficiency, the photomultiplier is used in fast photoelectric conversion and embedded processor is applied for signal processing. The specified parameters are given in Table 1.

In contrast to above numerical simulation, the experiment is on a closed-loop dynamic compensation. The image before compensation is shown in Fig. 9.

And after 1000 iterations, the energy tends to be more concentrated, the image on focal plane can be seen in Fig. 10.

The gray value distribution before and after compensation is shown in Fig. 11. We can see that the capability of energy focus has been obviously improved.

We can obtain the coupling efficiency variation through calculation of SR before and after compensation respectively. The results of SR before and after compensation are 6.05% and 30.59%.

After several experiments under different conditions, the images on focal plane are shown in Fig. 12, where Fig. 12(a) are

Table 1
Experiment parameters of FSO communication system.

Parameter	Value
Diameter of transmitter	20 mm
Diameter of receiver	20 mm
Laser wavelength	532 nm
Modulation frequency	1 kHz
Deformable mirrors unit number	32
Pixel size of CCD camera	5 μ m
Resolution of CCD camera	1024 \times 1024
Frames per second of CCD camera	30

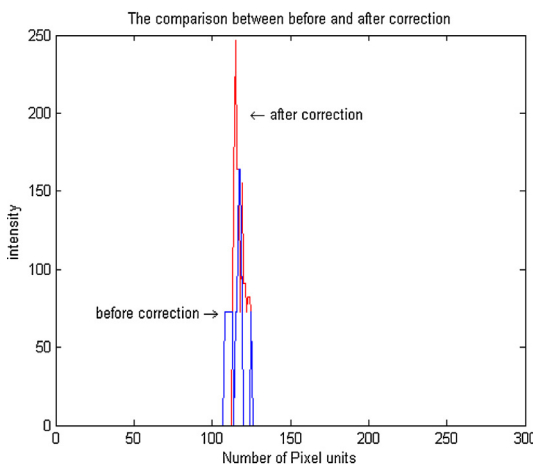


Fig. 11. Gray value distribution image (one-dimensional).

the images before compensation and Fig. 12(b) are the images after compensation. The experimental results are shown in Table 2.

As shown in Table 2, different turbulence strength causes different coupling efficiency variation before and after the compensation with the proposed algorithm. Through repeated experiments with different turbulence strength, we can see that the coupling

Table 2
Experiment results.

Coupling efficiency before compensation	Coupling efficiency after compensation
2.06%	20.51%
4.35%	28.32%
9.23%	31.20%
13.91%	35.96%

efficiency obviously increases demonstrating the validity of our method in atmospheric compensation in real time. In addition, first two groups of data show that the coupling efficiency can increase nearly from 3% to more than 20% when atmospheric turbulence is strong. The last two groups of data show that the coupling efficiency can only increase from nearly 10% to more than 30% when atmospheric turbulence is weak. The comparison indicates that the atmospheric compensation algorithm proposed here is working well in both weak and strong turbulence conditions.

6. Conclusion

In this paper, we compensate atmospheric turbulence with stochastic parallel gradient descent (SPGD) laser beam control algorithm in FSO communication systems. The analysis of the relationship between the coupling efficiency and Strehl rate is given. Different from the conventional wave-front conjugation principle-based AO systems, our SPGD algorithm does not need wave-front sensor as SH-WFS, which increases processing rate of the FSO system. The simulation and experimental results show that the coupling efficiency largely increases and the performance of FSO communication significantly improves.

In addition, further work about the relationship between the turbulence strength introduced by the turbulence simulation box and the structure constant of refractive index C_n^2 will be carried out in the near future.

Acknowledgment

This work was supported by the National Natural Science Foundation of China (No. 61171079).

References

- [1] X. Yi, Z. Liu, P. Yue, Optical scintillations statistics for FSO communications through moderate-to-strong non-Kolmogorov turbulence, *Opt. Laser Technol.* 47 (2013) 199–207.
- [2] A.W.M. van Eekeren, K. Schutte, J. Dijk, Turbulence compensation: an overview, *Proc. SPIE* 8355 (2012), 83550Q-1–83550Q-10.
- [3] S. Vyas, P. Senthilkumar, Two dimensional vortex lattices from pure wave-front tilts, *Opt. Commun.* 283 (2010) 2767–2771.
- [4] K. Murphy, D. Burke, N. Devaney, C. Dainty, Experimental detection of optical vortices with a Shack–Hartmann wavefront sensor, *Opt. Express* 18 (15) (2010) 15448–15460.
- [5] X. Fu, Z. Chen, Q. Guo, F. Pang, T. Wang, Beam reception and data transmission performance analysis of optical taper used in a mobile wireless optical communication, *Optik* 122 (2011) 1646–1649.
- [6] H. Song, R. Fraanje, G. Schitter, H. Kroese, G. Vdovin, M. Verhaegen, Model-based aberration correction in a closed-loop wavefront-sensor-less adaptive optics system, *Opt. Express* 18 (23) (2010) 24070–24084.
- [7] A. Zilberman, E. Golbraikh, N.S. Kopeika, Some limitations on optical communication reliability through Kolmogorov and non-Kolmogorov turbulence, *Opt. Commun.* 283 (2012) 1229–1235.
- [8] H. Takenaka, M. Toyoshima, Y. Takayama, Experimental verification of fiber-coupling efficiency for satellite-to-ground atmospheric laser downlinks, *Opt. Express* 20 (14) (2012) 15301–15308.
- [9] Y. Chen, L. Huang, L. Gan, Z. Li, Wavefront shaping of infrared light through a subwavelength hole, *Light Sci. Appl.* 1 (2012) e26.
- [10] J.I. Davis, Consideration of atmospheric turbulence in laser systems design, *Appl. Opt.* 5 (1) (1966) 139–147.
- [11] W. Liu, W. Shi, J. Cao, Bit error rate analysis with real-time pointing errors correction in free space optical communication systems, *Optik* (2013).

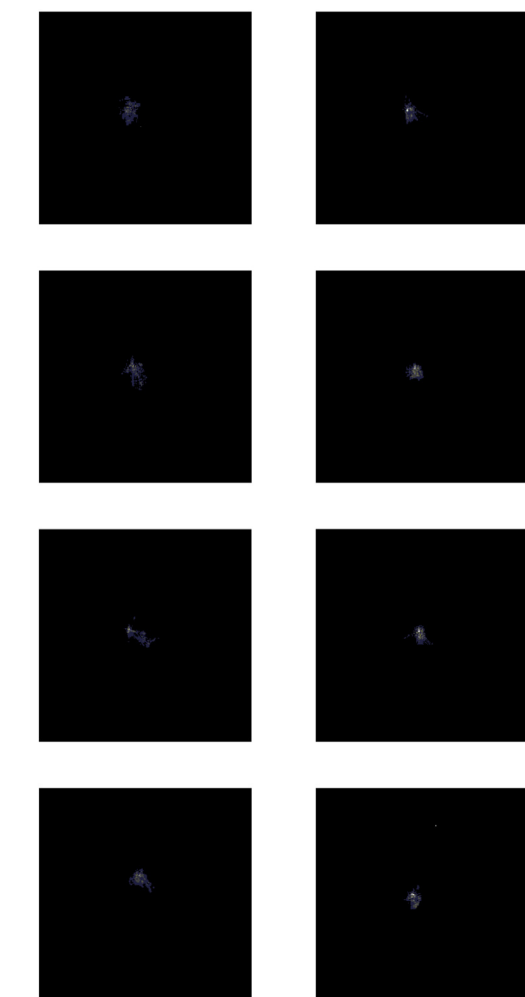


Fig. 12. Images on focal plane of several experiments.

- [12] N. Werth, M.S. Müller, J. Meier, A.W. Koch, Diffraction errors in micromirror-array based wavefront generation, *Opt. Commun.* 284 (9) (2011) 2317–2322.
- [13] N.K. Nahar, R.G. Rojas, Efficient free-space coupling to LMA-PCF by aberration correction, *IEEE Trans. Compon. Packag. Manuf. Technol.* 1 (10) (2011) 1553–1557 (october).
- [14] S. Jobling, K.T. McCusker, P.G. Kwiat, Adaptive Optics for Improved Mode-coupling Efficiencies, *OSA*, 2008 (19 October).
- [15] Y.M. Sabry, B. Saadany, D. Khalil, T. Bourouina, Silicon micromirrors with three-dimensional curvature enabling lensless efficient coupling of free-space light, *Light Sci. Appl.* 2 (2) (2013) e94.
- [16] Y. Dikmelik, D.M. Davidson, Fiber-coupling efficiency for free-space optical communication through atmospheric turbulence, *Appl. Opt.* 44 (23) (2005) 4946–4952.
- [17] Y. Zheng, X. Wang, L. Deng, F. Shen, X. Li, Experimental investigation of segmented adaptive optics for spatial laser array in an atmospheric turbulence condition, *Opt. Commun.* 284 (2011) 4975–4982.
- [18] M. Jiang, X. Zhang, C.A. Puliafito, H.F. Zhang, J. Shuiwang, Adaptive optics photoacoustic microscopy, *Opt. Express* 18 (21) (2010) 21770–21776.
- [19] G. Andersen, F. Ghebremichael, J. Baker, R. Gaddipati, P. Gaddipati, Holographic adaptive laser optics system, *SPIE* 8380 (D) (2012) 1–8.
- [20] J.H. Ali, A.E. Ali, A. Ali, A. Farid, Analysis of telescope array receivers for deep-space inter-planetary optical communication link between Earth and Mars, *Opt. Commun.* 283 (2010) 2032–2042.
- [21] W.O. Popoola, Z. Ghassemlooy, C.G. Lee, A.C. Boucouvalas, Scintillation effect on intensity modulated laser communication systems – a laboratory demonstration, *Opt. Laser Technol.* 42 (2010) 682–692.
- [22] T. Li, M. Gong, L. Huang, Y. Qiu, Q. Xue, Weighted Fried reconstructor and spatial-frequency response optimization of Shack–Hartmann wavefront sensing, *Appl. Opt.* 5 (29) (2012) 7115–7123.
- [23] V. Lin, H.-C. Wei, H.-T. Hsieh, J.-L. Hsieh, G.-D.J. Su, Design and fabrication of long-focal-length microlens arrays for Shack–Hartmann wavefront sensors, *Micro Nano Lett.* 6 (7) (2011) 523–526.
- [24] W. Liu, W. Shi, B. Wang, K. Yao, Y. Lv, J. Wang, Free space optical communication performance analysis with focal plane based wavefront measurement, *Opt. Commun.* 309 (2013) 212–220.
- [25] T. Weyrauch, M.A. Vorontsov, J.W. Gowens II, T.G. Bifano, Fiber coupling with adaptive optics for free-space optical communication, *SPIE* 4489 (2002) 177–184.
- [26] T. Weyrauch, M.A. Vorontsov, Atmospheric compensation with a speckle beacon in strong scintillation conditions: directed energy and laser communication applications, *Appl. Opt.* 44 (30) (2005) 6388–6401.
- [27] M.A. Vorontsov, G.W. Carhart, Adaptive phase-distortion correction based on parallel gradient-descent optimization, *Opt. Lett.* 22 (12) (2002) 907–909.
- [28] J.C. Spall, Multivariate stochastic approximation using a simultaneous perturbation gradient approximation, *IEEE Trans* 37 (3) (1992) 332–341.
- [29] R.J. Noll, Zernike polynomials and atmospheric turbulence, *J. Opt. Soc. Am.* 66 (3) (1976) 207–211.
- [30] H. Wu, H. Yan, X. Li, Modal correction for fiber-coupling efficiency in free-space optical communication systems through atmospheric turbulence, *Optik* 121 (19) (2010) 1789–1793.
- [31] T. Weyrauch, M.A. Vorontsov, J.W. Gowens II, T.G. Bifano, Fiber coupling with adaptive optics for free-space optical communication, *SPIE* 4489 (2002) 117–184.